



**HAL**  
open science

# Determination of Enantiomeric and Stable Isotope Ratio Fingerprints of Active Secondary Metabolites in Neroli (*Citrus aurantium* L.) Essential Oils for Authentication by Multidimensional Gas Chromatography and GC-C/P-IRMS

Aurélien Cuchet, Anthony Anchisi, Frédéric Schiets, Yohann Clément, Pierre Lantéri, Christelle Bonnefoy, Patrick Jame, Elise Carénini, Hervé Casabianca

## ► To cite this version:

Aurélien Cuchet, Anthony Anchisi, Frédéric Schiets, Yohann Clément, Pierre Lantéri, et al.. Determination of Enantiomeric and Stable Isotope Ratio Fingerprints of Active Secondary Metabolites in Neroli (*Citrus aurantium* L.) Essential Oils for Authentication by Multidimensional Gas Chromatography and GC-C/P-IRMS. *Journal of Chromatography B - Analytical Technologies in the Biomedical and Life Sciences*, 2021, pp.123003. 10.1016/j.jchromb.2021.123003 . hal-03403765

**HAL Id: hal-03403765**

**<https://hal.science/hal-03403765>**

Submitted on 5 Jan 2024

**HAL** is a multi-disciplinary open access archive for the deposit and dissemination of scientific research documents, whether they are published or not. The documents may come from teaching and research institutions in France or abroad, or from public or private research centers.

L'archive ouverte pluridisciplinaire **HAL**, est destinée au dépôt et à la diffusion de documents scientifiques de niveau recherche, publiés ou non, émanant des établissements d'enseignement et de recherche français ou étrangers, des laboratoires publics ou privés.



Distributed under a Creative Commons Attribution - NonCommercial 4.0 International License

1 **Determination of Enantiomeric and Stable Isotope Ratio Fingerprints of Active**  
2 **Secondary Metabolites in Neroli (*Citrus aurantium* L.) Essential Oils for**  
3 **Authentication by Multidimensional Gas Chromatography and GC-C/P-IRMS**

4 **Authors**

5 Aurélien Cuchet<sup>a,b,\*</sup>; Anthony Anchisi<sup>b</sup>; Frédéric Schiets<sup>b</sup>; Yohann Clément<sup>b</sup>; Pierre Lantéri<sup>b</sup>;  
6 Christelle Bonnefoy<sup>b</sup>, Patrick Jame<sup>b</sup>; Elise Carénini<sup>a</sup>; Hervé Casabianca<sup>b</sup>

7 **Affiliations**

8 <sup>a</sup>Albert Vieille SAS, 629 Route de Grasse, 06220 Vallauris, France

9 <sup>b</sup>Université de Lyon, CNRS, Université Claude Bernard Lyon 1, Institut des Sciences  
10 Analytiques, UMR 5280, 5 rue de la Doua, F-69100 Villeurbanne, France

11 **\*Corresponding author**

12 Aurélien Cuchet, aurelien.cuchet@isa-lyon.fr; aurelien.cuchet@gmail.com

13

14

15 **Abstract**

16 Neroli essential oil (EO), extracted from bitter orange blossoms, is one of the most expensive  
17 natural products on the market due to its poor yield and its use in fragrance compositions,  
18 such as cologne. Multiple adulterations of neroli EO are found on the market, and several  
19 authentication strategies, such as enantioselective gas chromatography (GC) and isotope ratio  
20 mass spectrometry (IRMS), have been developed in the last few years. However, neroli EO  
21 adulteration is becoming increasingly sophisticated, and analytical improvements are needed  
22 to increase precision. Enantiomeric and compound-specific isotopic profiling of numerous  
23 metabolites using multidimensional GC and GC-C/P-IRMS was carried out. These analyses  
24 proved to be efficient for geographical tracing, especially to distinguish neroli EO of Egyptian  
25 origin. In addition,  $\delta^2\text{H}$  values and enantioselective ratios can identify an addition of 10% of  
26 petitgrain EO. These results demonstrate that enantioselective and stable isotopic metabolite  
27 fingerprint determination is currently a necessity to control EOs.

28 **Keywords**

29 **Isotope ratio mass spectrometry, Multidimensional gas chromatography, Enantioselective**  
30 **analysis, Stable isotope analysis, Neroli essential oil, Authentication**

31

32

## 33 1. Introduction

34 The essential oil (EO) of neroli is produced via hydrodistillation or steam distillation of bitter  
35 orange (*Citrus aurantium* L.) blossoms. This EO is highly expensive due to its very low  
36 production yield (0.1%) [1]: at least one metric ton of fresh orange blossoms is required to  
37 produce only one kilogram of pure EO. The price of EO can fluctuate between 2,500 and 6,000  
38 €/kg depending on the country and the year. The quantity of EO produced worldwide is  
39 estimated between 4.5 to 6.5 MT per year. Neroli EO is nowadays an iconic product in the  
40 fragrance industry, due to its olfactive profile (Floral, orange blossom, green, methyl-like, and  
41 honeyed) in demand in the perfume industry [2]. Previous pharmacological studies have  
42 reported neurotonic properties [3] and antimicrobial, antioxidant [4,5], anticonvulsant [6],  
43 analgesic and anti-inflammatory activities [7] for this EO. Currently, this EO (*C. aurantium* ssp.  
44 *amara* var. *pumilla*) is mainly produced in Morocco, Tunisia, and Egypt but also in Spain, and  
45 Lebanon. The EO of another variety (*C. aurantium* L ssp *amara* var. *daidai*) is produced in  
46 China.

47 Adulteration is a common problem in the EO industry, especially with expensive EOs such as  
48 neroli. These adulterations are generally carried out to meet standard requirements, increase  
49 artificial EO quantities, or develop economic strategies. Orange blossom harvesting requires  
50 caution, and the production quality is a function of the weather and temperature conditions  
51 throughout the year. In the case of neroli EO, the main adulterations include blending with  
52 several known adulterations have been reported in the literature: blending with inexpensive  
53 EOs such as sweet orange EO (*Citrus sinensis*) [8], bitter orange EO [8], and petitgrain EO [9];  
54 addition of synthetic components such as linalool and linalyl acetate; and dilution with  
55 vegetable oils or solvents, such as sunflower oil [10] or ethanol [11].

56 Typical identification and characterization techniques, such as gas chromatography (GC)  
57 quality control or olfactive panel tests, cannot always differentiate a natural molecule from  
58 various origins (species or geographical) or a natural molecule from its synthetic equivalent.  
59 EO authentication requires the combination of several advanced analytical techniques to  
60 accurately identify adulteration with high precision. Currently, several methods are commonly  
61 used, such as the determination of synthetic residual impurities and natural markers [12],  
62 enantioselective analyses [13,14], radiocarbon activity assessment [12,15], and stable isotope  
63 analyses [12,13,16–19].

64 Enzymatic synthesis of asymmetric carbon molecules provides stereoselectivity. In most cases,  
65 one enantiomer is significantly in excess compared to the other enantiomer. However, organic  
66 synthesis will lead to a racemic mixture of both enantiomers. Adulteration of an EO can also  
67 be determined with a chiral study if some enantiomer proportions are reversed between the  
68 two EOs. Analysis of chiral molecules with enantioselective GC, monitored on cyclodextrin-  
69 based capillary columns, enables efficient determination of the enantiomeric ratios of  
70 compounds of interest. Chiral analysis is an effective tool to authenticate neroli EO purity.  
71 Several studies have been performed to determine the enantiomeric ratios of major  
72 metabolites in neroli EO, including linalool and linalyl acetate [14],  $\alpha$ -pinene,  $\beta$ -pinene,  
73 limonene [8,19], and other components [20].

74 Isotope ratio mass spectrometry (IRMS) is another powerful tool used to highlight the addition  
75 of synthetic molecules to an EO, blending with another natural extract, or assessment of its  
76 geographical origin. GC – combustion/pyrolysis – IRMS (GC-C/P-IRMS) allows for the  
77 determination of compound-specific  $\delta^{13}\text{C}$  and  $\delta^2\text{H}$  isotope ratios. IRMS has been recently used  
78 to identify adulterations of food products such as honey [21,22] or wine [23]. This analytical

79 technique is especially useful in the EO field, which presents complex matrices with several  
80 metabolites in nonnegligible quantities. GC-C/P-IRMS has been successfully used in the past  
81 for the authentication of several essential oils, including rose [17], oregano and thyme [24],  
82 *Allium* species [16], lemongrass and citronella [13], and lemon [18]. Several studies have also  
83 determined stable isotopic ratios on several secondary metabolites in neroli EOs, such as  
84 linalool and linalyl acetate [25], and other components ( $\beta$ -pinene, myrcene, limonene,  
85 terpinen-4-ol,  $\alpha$ -terpineol, nerol, neryl acetate, geranyl acetate,  $\beta$ -caryophyllene, (E)-  
86 nerolidol, and (E)-(E)-farnesol) [20,26].

87 In the present study, chiral and isotopic data of some compounds of neroli EOs have been  
88 used in combination with chemometrics to trace their geographical origin and to assess their  
89 authenticity. The first part of this study illustrates the use of these data to geographically  
90 discriminate neroli EO samples. Geographical traceability is relevant because an EO is defined  
91 by its extraction process, its species, and its location. Furthermore, prices vary with the  
92 geographical origin of harvest. The second part of this study is a focus on the purity of neroli  
93 EO samples. Although EO naturalness can be easily authenticated by  $^{14}\text{C}$  activity assessment  
94 or chiral studies, purity is much harder to detect, especially the addition of petitgrain EO,  
95 which is also manufactured from bitter orange. Petitgrain EO is obtained from the distillation  
96 process of bitter orange leaves and twigs. Neroli and petitgrain EOs are mainly composed of  
97 monoterpenic hydrocarbons and oxygenated monoterpenoids. The principal components of  
98 neroli and petitgrain EOs are linalool, limonene, linalyl acetate,  $\beta$ -pinene, (E)  $\beta$ -ocimene, (E)-  
99 nerolidol, (E) (E) farnesol, and  $\alpha$ -terpineol [27]. Neroli and petitgrain EOs share similar  
100 compounds, except for nitrogen-containing trace compounds (indole and methyl  
101 anthranilate), which have only been reported in neroli EO [28,29].

## 102 2. MATERIALS AND METHODS

### 103 2.1. Essential Oil Information

104 All studied samples (*C. aurantium* L ssp *amara* var. *pumilla*) were provided by Albert Vieille  
105 SAS (Vallauris, France). The traceability and provenance of the EOs were certified.

106 Neroli EOs came from Morocco (26 samples), Lebanon (4 samples), Tunisia (16 samples), and  
107 Egypt (22 samples) via several official producers.

108 In addition, Spanish samples (9 samples) were directly manufactured by Albert Vieille SAS from  
109 their aromatic raw material production facility localized in Sevilla region (Spain). Flowers of  
110 *Citrus aurantium* were mechanically harvested at the beginning of spring. Fresh flowers were  
111 manually sorted to remove leaves and twigs and quickly conveyed to production. Two  
112 different processes of distillation were undertaken. Steam distillation conditions applied were  
113 as follows: 1 ton of fresh flowers were loaded in a 4000 L still apparatus, with a water steam  
114 flow set between 100 and 150 L/h. After 3 hours of distillation, obtained yields comprised  
115 between 0.03 and 0.06%. Hydrodistillation conditions applied were as follows: 800 kg of fresh  
116 flowers were loaded in a 4000 L still apparatus, with a water flow set between 120 and 135  
117 L/h. After 3 hours of distillation, obtained yields comprised between 0.01 and 0.04%.

118 Petitgrain EOs were from Madagascar (3 samples) and Paraguay (6 samples). More  
119 information can be found in **Supplementary Table S1** including the year of production, harvest  
120 location details, the vegetative stage at time of harvest, and the extraction process.

### 121 2.2. Enantioselective Analyses

#### 122 2.2.1. Sample Preparation

123 Two hundred microliters of each EO sample were settled on silica gel 60A (35-70  $\mu\text{m}$  particle  
124 size, Carlo Erba Reagents, Val-de-Reuil, France). A primary fraction was collected by elution  
125 with 200 mL of pentane. This nonpolar fraction, largely composed of monoterpene and  
126 sesquiterpene molecules, was called Fraction 1. A second fraction was obtained by elution  
127 with 200 mL of diethyl ether. This polar fraction, mainly composed of alcohols and esters, was  
128 called Fraction 2. Fractions 1 and 2 were then evaporated with a rotary evaporator (Rotavapor  
129 R200, Büchi, Villebon-sur-Yvette, France) and diluted in 1 mL of hexane. This sample  
130 preparation was applied to dispose of 1-8 cineole from Fraction 1, which can interfere with  
131 limonene and  $\beta$ -phellandrene detection in Enantio-GC.

### 132 **2.2.2. Multidimensional Gas Chromatography (MDGC) Analyses**

133 MDGC analyses were performed on a 7890A GC gas chromatograph system (Agilent  
134 Technologies, Santa Clara, CA, USA) equipped with a flame ionization detector (FID) operating  
135 at a detector temperature of 250°C.

136 One microliter of each Fraction 1 was injected into the GC in split mode (120:1). Helium was  
137 used as the carrier gas with a constant inlet pressure of 26.4 psi. The flow rate was set to 0.7  
138 mL/min in the first column and 2 mL/min in the second column. Separation of volatile  
139 compounds was realized on an HP-1 primary capillary column (15 m x 0.200 mm x 0.5  $\mu\text{m}$  film  
140 thickness, Agilent Technologies) combined with a Dean Switch system (heart cutting program)  
141 with a second Cyclosil  $\beta$  column (30 m x 0.250 mm x 0.25  $\mu\text{m}$  film thickness, Agilent  
142 Technologies) coated with cyclodextrin stationary phase. The initial oven temperature was  
143 55°C held for 15 min, followed by an initial increase at 1°C/min to reach a temperature of 85°C.  
144 An additional increase in temperature at 10°C/min was then applied to reach a final  
145 temperature of 200°C and held for 10 min. Enantiomeric ratios were determined for  $\alpha$ -



146 thujene,  $\alpha$ -pinene, camphene, sabinene,  $\beta$ -pinene,  $\delta$ -3-carene, limonene, and  $\beta$ -phellandrene,  
147 as reported in **Figure 1a**.

148 An aliquot 0.2  $\mu$ L in volume of each Fraction 2 was injected into the GC in split mode (60:1).  
149 Helium was used as the carrier gas (18.8 psi applied inlet pressure). The flow rate was set to  
150 0.7 mL/min in the primary column and 1.7 mL/min in the secondary column. Separation of  
151 volatile compounds was realized on an HP-1 column (15 m x 0.200 mm x 0.5  $\mu$ m film thickness,  
152 Agilent Technologies) combined with a DEtTBuSilBetaCDX PS086 cyclodextrin stationary phase  
153 column (25 m\*0.25 mm\*0.25  $\mu$ m, Mega, Legano, Italy) and a Dean Switch system (heart  
154 cutting program). The oven temperature program was as follows: the initial temperature was  
155 held at 60°C for 5 min, increased at a rate of 1°C/min to reach a temperature of 95°C, and held  
156 for 9 min. An additional increase at 1°C/min was applied to reach 150°C. Then, a final increase  
157 at 10°C/min was carried out to reach 200°C, which was held for 10 min. Enantiomeric ratios  
158 were determined for linalool, terpinen-4-ol,  $\alpha$ -terpineol, linalyl acetate, and (E)-nerolidol, as  
159 reported in **Figure 1b**.

## 160 **2.3. Isotopic Analyses**

### 161 **2.3.1. Data Expression**

162 Isotopic results are expressed in delta ( $\delta$ ) units according to the following formula [30]:

$$163 \quad \delta^i E = \frac{(^i R_{Sample} - ^i R_{Reference})}{^i R_{Reference}}$$

164 where i is the mass number of the heavy isotope of element E,  $R_{Sample}$  is the isotope ratio of  
165 the sample, and  $R_{Reference}$  is the isotope ratio of a relevant internationally recognized reference  
166 material. The  $\delta$  values were multiplied by 1000 and are expressed in units "per mil" (‰).

167 High-purity gases of carbon dioxide (99.998%, 4.8 Messer) and hydrogen (99.999%, 5.0  
168 Messer) were used as the working reference gases injected with each sample. Helium  
169 (99.999% purity) was used as a carrier gas.

170 All studied metabolites in the EOs of interest were calibrated with a mixture of molecules ( $\beta$ -  
171 pinene, limonene, (E)- $\beta$ -ocimene, linalool, linalyl acetate,  $\alpha$ -terpineol, neryl acetate, geranyl  
172 acetate, nerol, geraniol, and (E)-nerolidol) purchased from Sigma Aldrich (Saint Louis, MO,  
173 USA) and TCI (Tokyo, Japan). These molecules were previously calibrated against international  
174 standards in elemental analysis – IRMS (EA-IRMS).

175 International reference materials IAEA CH7 (polyethylene foil:  $\delta^{13}\text{C}$  (‰) -32.15,  $\delta^2\text{H}$  (‰) -100)  
176 and USGS40 (L-glutamic acid:  $\delta^{13}\text{C}$  (‰) -26.39), supplied by the International Agency of Atomic  
177 Energy (IAEA, Vienna, Austria), were used to calibrate each molecule in the mixture, which  
178 allowed us to express our  $\delta^{13}\text{C}$  results relative to the Vienna Pee Dee Belemnite (VPDB) scale  
179 and our  $\delta^2\text{H}$  results relative to the Standard Mean Ocean Water (VSMOW) scale. Each sample  
180 was analyzed versus a monitoring gas for which two pulses were admitted with each analyte.  
181 All sample values were analyzed in duplicate and verified by bracketing the analytical  
182 sequence with international reference materials every six analyses. The  $\delta^{13}\text{C}$  values are  
183 expressed within a maximum standard deviation of  $\pm 0.28\text{‰}$  and those of  $\delta^2\text{H}$  within  $\text{SD} = \pm$   
184  $5\text{‰}$ .  $\delta^{13}\text{C}$  isotopic analyses of the standards molecules were conducted using a Flash HT  
185 elemental analyzer connected to a Delta V Plus via a Conflo V interface. The  $\delta^2\text{H}$   
186 measurements were carried out using a TC-EA elemental analyzer linked to a Delta V Plus via  
187 a Conflo V interface (all Thermo Fisher Scientific). The method is fully explained in a previous  
188 study [12]

189           **2.3.2. Gas Chromatography - Mass Spectrometry - Combustion/Pyrolysis - Isotope**  
190           **Ratio Mass Spectrometry (GC-MS-C/P-IRMS)**

191 The  $\delta^{13}\text{C}$  and  $\delta^2\text{H}$  values of targeted neroli and petitgrain EO metabolites were determined by  
192 GC-IRMS using a GC Trace 1310 simultaneously connected to an ISQ MS quadrupole mass  
193 spectrometer and to a Delta V Plus isotope ratio mass spectrometer via a GC Isolink II  
194 interface. (Thermo Fisher, Bremen, Germany). This equipment enabled the identification of  
195 compounds via the ISQ MS instrument and specific compound isotopic ratio measurements of  
196  $\delta^{13}\text{C}$  and  $\delta^2\text{H}$  via IRMS. Isotopic ratios were determined for  $\beta$ -pinene, limonene, (E)- $\beta$ -ocimene,  
197 linalool, linalyl acetate,  $\alpha$ -terpineol, neryl acetate, geranyl acetate, nerol, geraniol and (E)-  
198 nerolidol.

199 One microliter of diluted EO (1  $\mu\text{L}$  into 100  $\mu\text{L}$  of ethanol) was injected using a Tri Plus RSH  
200 autosampler in a Trace 1310 gas chromatograph equipped with an Agilent HP-Innowax column  
201 (60 m \* 0.250 mm \* 0.50  $\mu\text{m}$  internal diameter film thickness) used for chromatographic  
202 separation. The injection port was held at 250°C, fitted with a split liner containing glass wool  
203 and operated in split mode (120:1 for linalool and linalyl acetate assessment, 10:1 for the  
204 other compounds). The oven temperature program started at 60°C for 2 min, increased to  
205 100°C at a rate of 2°C/min, increased to 150°C at a rate of 5°C/min, increased to 200°C at a  
206 rate of 2°C/min, and increased to 260°C at a rate of 1°C/min (which was for 5 min).  
207 Components were separated at a flow rate of 1.2 mL/min and divided in 2 ways using a Sil  
208 Flow connector.

209 The combustion of carbon in carbon dioxide was achieved using an alumina tube containing  
210 nickel oxide maintained at 1000°C in a furnace. Pyrolysis of the sample for  $^2\text{H}$  measurement in  
211  $\text{H}_2$  was carried out at a high temperature (1400°C) using an alumina conversion tube (Thermo

212 Fischer Scientific). Undecane,  $C_{11}H_{24}$  (Sigma Aldrich), was regularly added to regenerate the  
213 alumina pyrolysis tube.

#### 214 **2.4. Statistical analysis**

215 Multivariate statistical analyses were performed using R version 4.0.3 (R Core Team, Vienna,  
216 Austria) [31] with corrplot [32], ropls [33], Factoextra [34], and FactoMiner [35] packages. The  
217 Pearson correlation test was carried out to determine pairwise correlations between isotope  
218 ratio values. Univariate analysis was realized to determine significant differences between  
219 species, within a confidence level  $p$ -value  $< 0.05$ .

220 For multivariate data analyses, data were first analysed with unsupervised method such as  
221 principal component analysis (PCA) [36] and clustering. PCA was used in this study to describe  
222 and to assess the quality and homogeneity of the 90 samples of interest (81 neroli EO and 9  
223 petitgrain EO). An autoscaling was realized prior to PCA and Ward's minimum variance  
224 clustering method was applied to perform the hierarchical clustering [34].

225 Supervised methods were then carried out, including orthogonal partial least square–  
226 discriminant analysis (OPLS-DA), to link models and variables responsible for the separation  
227 observed on the unsupervised method [37].

228 A 7-fold stratified cross validation was repeated 50 times to avoid overfitting the small number  
229 of data-points. Features were ranked according to the variable importance projection (VIP)  
230 from OPLS-DA. S-plot verifies the selectivity and the specificity of the selected features. The  
231 model's quality was evaluated based on the residuals ( $R^2X$ ,  $R^2Y$ ) and the models predictive  
232 ability parameter ( $Q^2_{cum}$ ) [38]. The statistical significances of models were also assessed using  
233 confusion matrix.

### 234 3. Results and Discussion

#### 235 3.1. Enantiomeric Ratio Fingerprint

##### 236 3.1.1. Neroli Essential Oils

237 Enantiomeric ratio determination was conducted in this study to minor chiral compounds in  
238 neroli EOs to obtain a complete enantiomeric signature of the studied EOs to improve  
239 authentication. This study was achieved using a MDGC approach. This technique was  
240 previously applied to authenticate other EOs, such as rosemary EO [39]. Thirteen chiral  
241 components were identified in the EO:  $\alpha$ -thujene,  $\alpha$ -pinene, camphene,  $\beta$ -pinene,  $\delta$ -3-carene,  
242 sabinene, limonene,  $\beta$ -phellandrene, linalool, linalyl acetate, terpinen-4-ol,  $\alpha$ -terpineol, and  
243 (E)-nerolidol.

244 The results are depicted in **Table 1**. The neroli EOs from Morocco, Tunisia and Lebanon showed  
245 the same chiral profile with the dominance of levorotary (-) form:  $\alpha$ -thujene,  $\alpha$ -pinene,  
246 camphene, sabinene,  $\beta$ -pinene,  $\delta$ -3-carene,  $\beta$ -phellandrene, linalool, linalyl acetate, and  
247 terpinen-4-ol. Limonene,  $\alpha$ -terpineol, and (E)-nerolidol were predominantly dextrorotary (+).  
248 The  $\alpha$ -pinene,  $\beta$ -pinene, limonene, linalool, linalyl acetate, terpinene-4-ol,  $\alpha$ -terpineol and (E)-  
249 nerolidol chiral results were in good agreement with those of previous enantioselective  
250 studies of neroli EOs [8,14,19].

251 Several samples from Egypt featured different chiral signatures: racemization of  $\alpha$ -pinene and  
252  $\beta$ -phellandrene was observed, and reversions of sabinene and terpinen-4-ol enantiomer  
253 amounts were also detected. These results were in good agreement with those found in the  
254 literature [20], except for a contradiction with the  $\alpha$ -terpineol enantiomeric ratio previously  
255 indicated in the literature, as we reported the R enantiomer as the major enantiomer. These  
256 results suggest differences in varieties between neroli EO samples from Egypt and other

257 geographical origins. It is also hypothesized that Egyptian samples were produced from  
258 flowers of a citrus hybrid *aurantium x sinensis*, based on our harvested area data. Sweet  
259 orange *Citrus sinensis* cultivars are the most widely grown among *Citrus* species in Egypt  
260 (accounting for 69% of the total cultivated area) [40] and bitter orange *Citrus aurantium* tree  
261 is the main *Citrus* rootstock used in Egypt.

262 Several enantiomeric discrepancies were detected for minor compounds ( $\alpha$ -pinene, sabinene,  
263 terpinen-4-ol, and  $\beta$ -phellandrene), which were all present at less than 2% of the total  
264 composition of neroli EOs. Differences between neroli EOs of Egyptian and other origins would  
265 have been undetected if only chiral analyses of major compounds were conducted. This  
266 highlights the interest in carrying out a complete enantiomeric profiling approach to  
267 authenticate EOs. These results are compelling, as neroli EOs from Egypt also present  
268 perceptible olfactive profiles. Indeed, EO is more fresh, lemony, and less methylated than  
269 Morocco origin and more green and less honeyed than Tunisian.

### 270 **3.1.2. Petitgrain Essential Oils**

271 Petitgrain EO is a common adulterant in neroli EO. This adulteration can be unintentional if  
272 producers are not meticulous enough during harvest, as they must harvest only flowers of *C.*  
273 *aurantium* and not the leaves. It can be tricky to detect such adulterations, as major  
274 compounds, including linalool and linalyl acetate, are similar between the two types of  
275 hydrodistilled *C. aurantium* EOs. Enantiomeric fingerprints of chiral metabolites can also  
276 highlight EO blending. Several studies have established chiral databases on petitgrain, sweet,  
277 and bitter orange EOs [8,19,41]. By comparison with chiral data for sweet orange and bitter  
278 orange EOs, adulteration of neroli EO can be detected. However, literature databases suggest  
279 that the petitgrain chiral profile is similar to that of neroli.

280 The petitgrain EO chiral signature is detailed in Table 1. Enantiomeric ratios were determined  
281 in 9 samples from Madagascar and Paraguay.  $\alpha$ -pinene,  $\beta$ -pinene, limonene, linalool, linalyl  
282 acetate, terpinen-4-ol, and  $\alpha$ -terpineol chirality were consistent with previous investigations  
283 [8,19,42].

284 No significant differences were observed between petitgrain and neroli profiling, except for  
285 limonene and nerolidol (+) forms, which were less predominant in the petitgrain profile than  
286 in the neroli profile. Enantiomeric profiles of petitgrain and neroli EOs are not sufficiently  
287 distinct to highlight an addition of petitgrain EO in neroli EO. A complementary analysis is  
288 required to detect such adulteration.

### 289 3.2. $\delta^{13}\text{C}$ and $\delta^2\text{H}$ Isotopic Composition

290 Multiple isotope ( $^{13}\text{C}$  and  $^2\text{H}$ ) analysis of multiple components results in a large amount of  
291 information about the samples: compound-specific isotope analysis with GC-C/P-IRMS  
292 enables the assessment of the complete isotope fingerprint of neroli EO samples via  
293 determination of the  $\delta^{13}\text{C}$  and  $\delta^2\text{H}$  ratios of major metabolites.

294 Carbon isotope ratios are dependent on the metabolic pathways for carbon fixation in  
295 photosynthesis. *C. aurantium* is a C3 plant (Calvin cycle [43]). Its  $\delta^{13}\text{C}$  is between -20 and -33  
296 ‰ [44]. By comparison, a C4 plant (Hatch and Slack pathway [45]), such as lemongrass [13],  
297 has a  $\delta^{13}\text{C}$  value slightly more positive, between -9 and -16 ‰ [46]. The  $\delta^{13}\text{C}$  stable isotopic  
298 ratios of several metabolites of the samples are detailed in **Table 2**. These values are in line  
299 with the C3 plant range stated in the literature. The results were also consistent with those of  
300 previous  $\delta^{13}\text{C}$  analyses conducted with neroli EOs [20]. Furthermore, the results were not  
301 significantly different among geographical origins. It was expected that all the samples were  
302 neroli EOs and came from the same *C. aurantium* natural plant variety.

303 Hydrogen isotopic ratios are predominantly influenced by the geographical origin of a plant  
304 due to the hydrological cycle [47], resulting in  $\delta^2\text{H}$  being dependent on the geographical area.  
305 Neroli EO  $\delta^2\text{H}$  values are detailed in **Table 3**. Several differences were observed among the  
306 different geographical origins. It is important to note that the samples from Egypt were  
307 different than other samples, with mean  $\delta^2\text{H}$  values higher than those of samples with other  
308 origins. According to Hör et al. (2001) [25], neroli EOs have  $\delta^2\text{H}$  values (measured in 4 samples)  
309 ranging between -234‰ and -253‰ for linalool and -270‰ and -272‰ for linalyl acetate. In  
310 this study,  $\delta^2\text{H}$  values of the 86 samples were higher than the previously reported values, with  
311 mean values between -200‰ (Egypt) and -214‰ (Tunisia) for linalool and between -218‰  
312 (Egypt) and -240‰ (Tunisia) for linalyl acetate.

313 In conclusion, compound-specific stable isotopic data are relevant because they provide a  
314 stable isotopic fingerprint that provides geographical information, as the samples from Egypt  
315 were clearly different than those from Morocco, Lebanon, and Tunisia.

### 316 **3.3. Chemometric Analyses**

#### 317 **3.3.1. Geographical Origin Authentication**

318 Principal component analysis (PCA) was carried out on the entire sample data set (83 samples  
319 of neroli), with 33 parameters as variables (enantiomeric ratios and  $\delta^{13}\text{C}$  and  $\delta^2\text{H}$  isotopic  
320 ratios) to obtain a visual representation of the collected data (**Figure 2a**). Two different  
321 clusters could be observed: one comprising neroli EOs from Morocco, Lebanon, and Tunisia,  
322 and another including neroli EOs from Egypt. Most Spanish samples were in the first cluster,  
323 but two commercial samples were found in the second cluster. The Moroccan and Tunisian  
324 samples were also slightly separated from each other.



325 Hierarchical clustering was then realized to distinguish the clusters with more accuracy. This  
326 clustering technique calculates the difference in distance between each sample. The cluster  
327 plot (**Figure 2b**) helps to distinguish three different clusters: one comprising samples from  
328 Spain, Morocco, Tunisia, and Lebanon (Cluster 1) and two clusters including samples from  
329 Egypt (Clusters 2 and 3). Both Egyptian clusters corresponded to different providers.  
330 Geographical location differences might explain these differences: Cluster 2 includes only  
331 samples from the specific Egyptian region of Gharbia Governorate, whereas Cluster 3 regroups  
332 other samples from Egypt.

333 As described in **Supplementary Table S1**, neroli essential oils were extracted from two  
334 different several processes: steam distillation and hydrodistillation. Based on the clustering,  
335 the extraction process does not affect the enantiomeric and isotopic compositions, as no  
336 differences were observed between steam distilled and hydrodistilled samples. The vegetative  
337 stage at time of harvest, the type of resources (wild or cultivated flowers), and the year of  
338 production do not impact chirality and isotopy of neroli EO metabolites too.

339 This study highlights the differences in quality between Egyptian and other neroli EOs.  
340 Authentication criteria need to be different among the two groups of EO samples to avoid  
341 misinterpreting analytical results from Egypt samples.

### 342 **3.3.2. Purity Authentication**

343 An additional PCA process was employed, this time including petitgrain samples. **Figure 3a**  
344 depicts the score plot of the principal components F1 and F2, which accounted for 49% of the  
345 total variance in the data. Differences between neroli and petitgrain EOs were successfully  
346 visualized.

347 Orthogonal partial least squares – discriminant analysis (OPLS-DA) was conducted to identify  
348 discriminant variables. This model was built from all samples using all parameters. The  
349 projection of the individual samples is represented in **Figure 3b**: neroli and petitgrain are  
350 significantly separated on the OPLS-DA score plot. The S-Plot visualization represented in  
351 **Figure 3c** highlights discriminant variables. The S-plot represents the variable confidence  
352 (correlation) against the variable contribution (covariance). Variables with the highest  
353 contributions and reliability are  $\delta^2\text{H}$  stable isotope values, including nerol, geranyl acetate,  
354 geraniol, and  $\alpha$ -terpineol. The geographical origins of petitgrain samples (Madagascar,  
355 Paraguay) probably affecting this discrimination, but this large isotopic fractionation is also  
356 explained by the differences between leaves and flowers. (E)-Nerolidol and limonene  
357 enantiomeric distributions also present high contributions. The  $\delta^{13}\text{C}$  parameter did not seem  
358 to contribute to clustering based on this S-Plot representation.

359 Finally, petitgrain was added to one Moroccan neroli EO sample. Three levels of adulteration  
360 were applied (10%, 20%, and 50% adulteration). PCA (**Figure 4**) was then performed to  
361 observe the effects of this addition on the data. Since neroli EOs presented geographical  
362 variations, as seen earlier, only Moroccan samples were represented. As observed in the  
363 figure, adulterated samples were no longer in the neroli cluster. Even 10% adulteration can  
364 be detected with the determination of enantiomeric and stable isotope ratio fingerprints of  
365 the major metabolites of neroli EO.

366 This study shows the importance of determining the most complete enantiomeric and isotopic  
367 signature to investigate adulterations, especially if the matrices are similar to those of neroli  
368 and petitgrain EOs.

369 **Conclusion**

370 Measurements of enantiomeric and isotopic ratios of major metabolites of neroli essential oils  
371 were performed using MDGC and GC-C/P-IRMS. The data banks were treated with  
372 chemometric models, leading to geographical and authentication of varieties.

373 Geographical discrimination was achieved using PCA and hierarchical clustering models.

374 We demonstrated that an adulteration of 10% of petitgrain could be highlighted in neroli  
375 essential oil.

376 The work carried out in this study highlighted the interest to use simultaneously enantiomeric  
377 and isotopic compound-specific analyses to authenticate geographical and botanical origins  
378 of an essential oil sample. This type of multianalytical approach can be reproduced to other  
379 type of complex essential oils in the future to improve authentication and detect fraudulent  
380 products.

### 381 **Acknowledgments**

382 This work was conducted in partial fulfilment of the PhD requirements for Aurélien Cuchet  
383 who received a grant from the Association Nationale de la Recherche et de la Technologie  
384 (ANRT, Paris, France). The research was supported by a contract between Albert Vieille SAS  
385 and ISA (Institut des Sciences Analytiques, Villeurbanne, France).

386 **References**

- 387 [1] L. Peyron, Peyron, L., 2002. Medicinal and Aromatic Plants, Industrial Profiles. 26, p.148,  
388 in: 2002.
- 389 [2] R.G. Berger, ed., Flavours and fragrances: chemistry, bioprocessing and sustainability,  
390 Springer, Berlin ; New York, 2007.
- 391 [3] L. Duval, Les huiles essentielles à l'officine, UFR de Medecine et de Pharmacie de Rouen,  
392 2012. <https://dumas.ccsd.cnrs.fr/dumas-00713158>.
- 393 [4] H. Değirmenci, H. Erkurt, Relationship between volatile components, antimicrobial and  
394 antioxidant properties of the essential oil, hydrosol and extracts of *Citrus aurantium* L.  
395 flowers, *J. Infect. Public Health.* 13 (2020) 58–67.  
396 <https://doi.org/10.1016/j.jiph.2019.06.017>.
- 397 [5] N. Dosoky, W. Setzer, Biological Activities and Safety of Citrus spp. Essential Oils, *Int. J.*  
398 *Mol. Sci.* 19 (2018) 1966. <https://doi.org/10.3390/ijms19071966>.
- 399 [6] T. Azanchi, H. Shafaroodi, J. Asgarpanah, Anticonvulsant activity of *Citrus aurantium*  
400 blossom essential oil (neroli): involvement of the GABAergic system, *Nat. Prod. Commun.*  
401 9 (2014) 1615–1618.
- 402 [7] P. Khodabakhsh, H. Shafaroodi, J. Asgarpanah, Analgesic and anti-inflammatory activities  
403 of *Citrus aurantium* L. blossoms essential oil (neroli): involvement of the nitric  
404 oxide/cyclic-guanosine monophosphate pathway, *J. Nat. Med.* 69 (2015) 324–331.  
405 <https://doi.org/10.1007/s11418-015-0896-6>.
- 406 [8] G. Dugo, L. Mondello, eds., Citrus oils: composition, advanced analytical techniques,  
407 contaminants, and biological activity, CRC Press, Boca Raton, FL, 2011.
- 408 [9] W.A. König, D.H. Hochmuth, Enantioselective Gas Chromatography in Flavor and  
409 Fragrance Analysis: Strategies for the Identification of Known and Unknown Plant  
410 Volatiles, *J. Chromatogr. Sci.* 42 (2004) 423–439.  
411 <https://doi.org/10.1093/chromsci/42.8.423>.
- 412 [10] W. Mbogning Feudjio, H. Ghalila, M. Nsangou, Y. Majdi, Y. Mbesse Kongbonga, N.  
413 Jaïdane, Fluorescence Spectroscopy Combined with Chemometrics for the Investigation  
414 of the Adulteration of Essential Oils, *Food Anal. Methods.* 10 (2017) 2539–2548.  
415 <https://doi.org/10.1007/s12161-017-0823-4>.
- 416 [11] R. Singhal, P. Kulkarni, D. Rege, Quality indices for spice essential oils, in: *Handb. Herbs*  
417 *Spices*, CRC Press, Boca Raton, 2001: pp. 22–23.
- 418 [12] A. Cuchet, P. Jame, A. Anchisi, F. Schiets, C. Oberlin, J.-C. Lefèvre, E. Carénini, H.  
419 Casabianca, Authentication of the naturalness of wintergreen (*Gaultheria* genus)  
420 essential oils by gas chromatography, isotope ratio mass spectrometry and radiocarbon  
421 assessment, *Ind. Crops Prod.* 142 (2019) 10.  
422 <https://doi.org/10.1016/j.indcrop.2019.111873>.

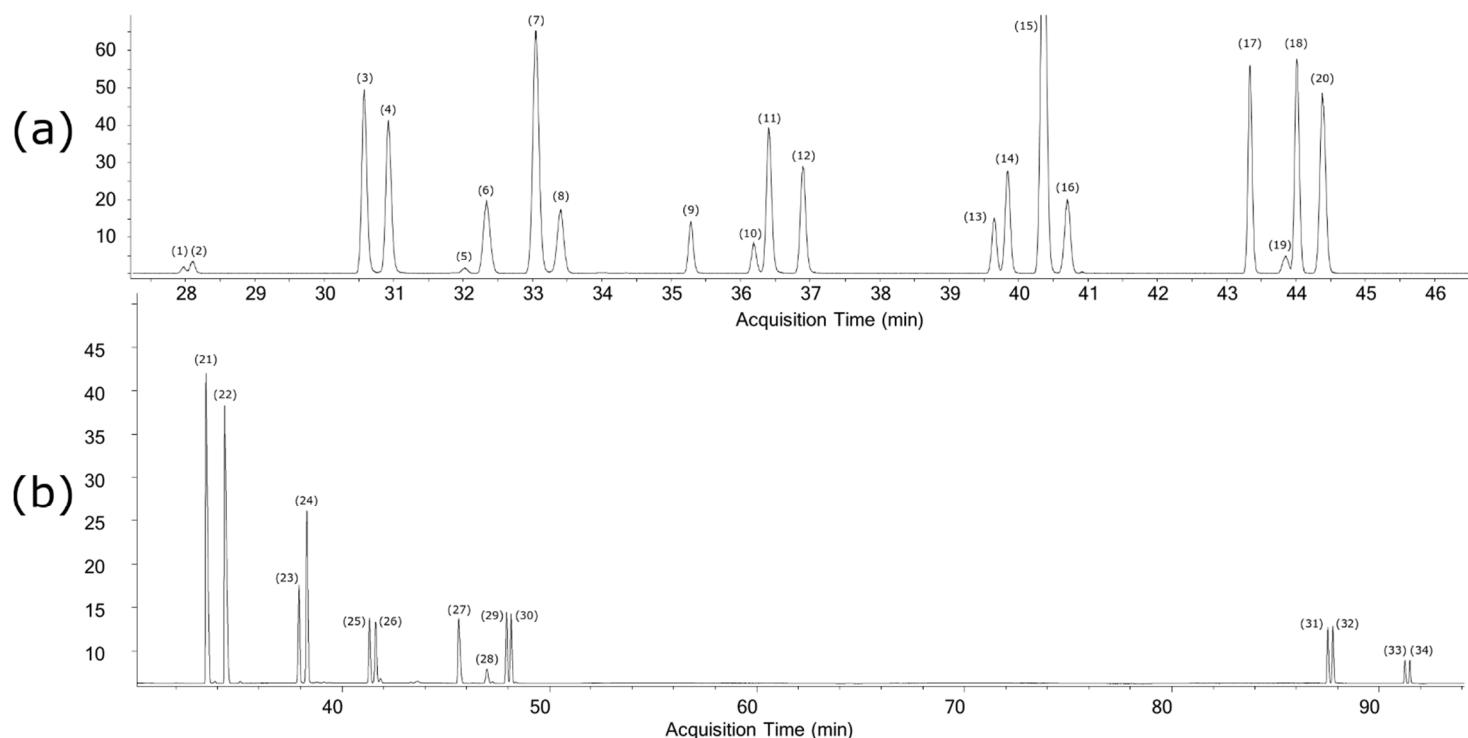
- 423 [13] T.-T. Nhu-Trang, H. Casabianca, M.-F. Grenier-Loustalot, Authenticity control of essential  
424 oils containing citronellal and citral by chiral and stable-isotope gas-chromatographic  
425 analysis, *Anal. Bioanal. Chem.* 386 (2006) 2141–2152. [https://doi.org/10.1007/s00216-](https://doi.org/10.1007/s00216-006-0842-2)  
426 006-0842-2.
- 427 [14] H. Casabianca, J.B. Graff, V. Faugier, F. Fleig, C. Grenier, Enantiomeric Distribution Studies  
428 of Linalool and Linalyl Acetate. A Powerful Tool for Authenticity Control of Essential Oils,  
429 *J. High Resolut. Chromatogr.* 21 (1998) 107–112. [https://doi.org/10.1002/\(SICI\)1521-](https://doi.org/10.1002/(SICI)1521-4168(19980201)21:2<107::AID-JHRC107>3.0.CO;2-A)  
430 4168(19980201)21:2<107::AID-JHRC107>3.0.CO;2-A.
- 431 [15] H. Gershon, A. Lykkeberg, F. Goren, S. Mason, Identifying Fraudulent Natural Products:  
432 A Perspective on the Application of Carbon-14 Analysis, *J. Agric. Food Chem.* 67 (2019)  
433 13393–13399. <https://doi.org/10.1021/acs.jafc.9b01821>.
- 434 [16] A. Cuchet, A. Anchisi, P. Telouk, Y. Yao, F. Schiets, F. Fourel, Y. Clément, P. Lantéri, E.  
435 Carénini, P. Jame, H. Casabianca, Multi-element (<sup>13</sup>C, <sup>2</sup>H and <sup>34</sup>S) bulk and compound-  
436 specific stable isotope analysis for authentication of *Allium* species essential oils, *Food*  
437 *Control.* 126 (2021) 108086. <https://doi.org/10.1016/j.foodcont.2021.108086>.
- 438 [17] F. Pellati, G. Orlandini, K.A. van Leeuwen, G. Anesin, D. Bertelli, M. Paolini, S. Benvenuti,  
439 F. Camin, Gas chromatography combined with mass spectrometry, flame ionization  
440 detection and elemental analyzer/isotope ratio mass spectrometry for characterizing  
441 and detecting the authenticity of commercial essential oils of *Rosa damascena* Mill.:  
442 GC/MS, GC/FID and GC/C/IRMS analysis of *Rosa damascena* essential oil, *Rapid Commun.*  
443 *Mass Spectrom.* 27 (2013) 591–602. <https://doi.org/10.1002/rcm.6489>.
- 444 [18] L. Schipilliti, P. Dugo, I. Bonaccorsi, L. Mondello, Authenticity control on lemon essential  
445 oils employing Gas Chromatography–Combustion-Isotope Ratio Mass Spectrometry  
446 (GC–C-IRMS), *Food Chem.* 131 (2012) 1523–1530.  
447 <https://doi.org/10.1016/j.foodchem.2011.09.119>.
- 448 [19] A. Mosandl, Enantioselective capillary gas chromatography and stable isotope ratio mass  
449 spectrometry in the authenticity control of flavors and essential oils, *Food Rev. Int.* 11  
450 (1995) 597–664. <https://doi.org/10.1080/87559129509541063>.
- 451 [20] I. Bonaccorsi, D. Sciarrone, L. Schipilliti, A. Trozzi, H.A. Fakhry, G. Dugo, Composition of  
452 Egyptian neroli oil, *Nat. Prod. Commun.* 6 (2011) 1009–1014.
- 453 [21] H. Dong, K. Xiao, Y. Xian, Y. Wu, Authenticity determination of honeys with non-  
454 extractable proteins by means of elemental analyzer (EA) and liquid chromatography (LC)  
455 coupled to isotope ratio mass spectroscopy (IRMS), *Food Chem.* 240 (2018) 717–724.  
456 <https://doi.org/10.1016/j.foodchem.2017.08.008>.
- 457 [22] H. Dong, D. Luo, Y. Xian, H. Luo, X. Guo, C. Li, M. Zhao, Adulteration Identification of  
458 Commercial Honey with the C-4 Sugar Content of Negative Values by an Elemental  
459 Analyzer and Liquid Chromatography Coupled to Isotope Ratio Mass Spectroscopy, *J.*  
460 *Agric. Food Chem.* 64 (2016) 3258–3265. <https://doi.org/10.1021/acs.jafc.6b00691>.

- 461 [23] H. Wu, L. Tian, B. Chen, B. Jin, B. Tian, L. Xie, K.M. Rogers, G. Lin, Verification of imported  
462 red wine origin into China using multi isotope and elemental analyses, *Food Chem.* 301  
463 (2019) 125137. <https://doi.org/10.1016/j.foodchem.2019.125137>.
- 464 [24] T.-T. Nhu-Trang, H. Casabianca, M.-F. Grenier-Loustalot, Deuterium/hydrogen ratio  
465 analysis of thymol, carvacrol,  $\gamma$ -terpinene and *p*-cymene in thyme, savory and oregano  
466 essential oils by gas chromatography–pyrolysis–isotope ratio mass spectrometry, *J.*  
467 *Chromatogr. A.* 1132 (2006) 219–227. <https://doi.org/10.1016/j.chroma.2006.07.088>.
- 468 [25] K. Hör, C. Ruff, B. Weckerle, T. König, P. Schreier, Flavor Authenticity Studies by  $^2\text{H}/^1\text{H}$   
469 Ratio Determination Using On-line Gas Chromatography Pyrolysis Isotope Ratio Mass  
470 Spectrometry, *J. Agric. Food Chem.* 49 (2001) 21–25. <https://doi.org/10.1021/jf000829x>.
- 471 [26] A. Mosandl, D. Juchelka, Advances in the Authenticity Assessment of Citrus Oils, *J. Essent.*  
472 *Oil Res.* 9 (1997) 5–12. <https://doi.org/10.1080/10412905.1997.9700706>.
- 473 [27] O. Boussaada, R. Chemli, Chemical Composition of Essential Oils from Flowers, Leaves  
474 and Peel of *Citrus aurantium L. var. amara* from Tunisia, *J. Essent. Oil Bear. Plants.* 9  
475 (2006) 133–139. <https://doi.org/10.1080/0972060X.2006.10643484>.
- 476 [28] D. De Rovira, Dictionary of Flavors, 3rd Edition, Wiley.Com. (2017).  
477 [https://www.wiley.com/en-fr/Dictionary+of+Flavors%2C+3rd+Edition-p-](https://www.wiley.com/en-fr/Dictionary+of+Flavors%2C+3rd+Edition-p-9781118856413)  
478 [9781118856413](https://www.wiley.com/en-fr/Dictionary+of+Flavors%2C+3rd+Edition-p-9781118856413) (accessed January 10, 2019).
- 479 [29] A.M. Grumezescu, A.M. Holban, Soft Chemistry and Food Fermentation, in: 2017.
- 480 [30] W.A. Brand, T.B. Coplen, J. Vogl, M. Rosner, T. Prohaska, Assessment of international  
481 reference materials for isotope-ratio analysis (IUPAC Technical Report), *Pure Appl. Chem.*  
482 86 (2014) 425–467. <https://doi.org/10.1515/pac-2013-1023>.
- 483 [31] R Core Team, R: A Language and Environment for Statistical Computing, R Foundation for  
484 Statistical Computing, Vienna, Austria, 2020. <https://www.R-project.org/>.
- 485 [32] T. Wei, V. Simko, R package “corrplot”: Visualization of a Correlation Matrix, 2017.  
486 <https://github.com/taiyun/corrplot>.
- 487 [33] E.A. Thévenot, A. Roux, Y. Xu, E. Ezan, C. Junot, Analysis of the Human Adult Urinary  
488 Metabolome Variations with Age, Body Mass Index, and Gender by Implementing a  
489 Comprehensive Workflow for Univariate and OPLS Statistical Analyses, *J. Proteome Res.*  
490 14 (2015) 3322–3335. <https://doi.org/10.1021/acs.jproteome.5b00354>.
- 491 [34] A. Kassambara, F. Mundt, factoextra: Extract and Visualize the Results of Multivariate  
492 Data Analyses, 2020. <https://CRAN.R-project.org/package=factoextra>.
- 493 [35] S. Lê, J. Josse, F. Husson, FactoMineR: An R Package for Multivariate Analysis, *J. Stat.*  
494 *Softw.* 25 (2008) 1–18. <https://doi.org/10.18637/jss.v025.i01>.
- 495 [36] I.T. Jolliffe, Principal Component Analysis - Second Edition, Springer Ser. Stat. (2002).  
496 <https://doi.org/10.1007/b98835>.

- 497 [37] M. Tenenhaus, *La régression PLS: théorie et pratique*, Editions TECHNIP, 1998.
- 498 [38] A. Levet, C. Bordes, Y. Clément, P. Mignon, H. Chermette, P. Marote, C. Cren-Olivé, P.  
499 Lantéri, Quantitative structure–activity relationship to predict acute fish toxicity of  
500 organic solvents, *Chemosphere*. 93 (2013) 1094–1103.  
501 <https://doi.org/10.1016/j.chemosphere.2013.06.002>.
- 502 [39] L. Mondello, A. Casilli, P.Q. Tranchida, M. Furukawa, K. Komori, K. Miseki, P. Dugo, G.  
503 Dugo, Fast enantiomeric analysis of a complex essential oil with an innovative  
504 multidimensional gas chromatographic system, *J. Chromatogr. A*. 1105 (2006) 11–16.  
505 <https://doi.org/10.1016/j.chroma.2005.08.013>.
- 506 [40] W.F. Abobatta, *Citrus Varieties in Egypt: An Impression*, *Int. Res. J. Appl. Sci.* (2019) 4.
- 507 [41] I. Bonaccorsi, D. Sciarrone, A. Cotroneo, L. Mondello, P. Dugo, G. Dugo, Enantiomeric  
508 distribution of key volatile components in Citrus essential oils, *Rev. Bras. Farmacogn.* 21  
509 (2011) 841–849. <https://doi.org/10.1590/S0102-695X2011005000123>.
- 510 [42] D. Juchelka, A. Steil, K. Witt, A. Mosandl, Chiral Compounds of Essential Oils. XX. Chirality  
511 Evaluation and Authenticity Profiles of Neroli and Petitgrain Oils, *J. Essent. Oil Res.* 8  
512 (1996) 487–497. <https://doi.org/10.1080/10412905.1996.9700674>.
- 513 [43] M. Calvin, J.A. Bassham, *The Photosynthesis of Carbon Compounds*, Benjamin, New York,  
514 1962. <https://doi.org/10.2172/910351>.
- 515 [44] M.H. O’Leary, Carbon Isotopes in Photosynthesis, *BioScience*. 38 (1988) 328–336.  
516 <https://doi.org/10.2307/1310735>.
- 517 [45] M.D. Hatch, C.R. Slack, Photosynthetic CO<sub>2</sub>-Fixation Pathways, *Annu. Rev. Plant Physiol.*  
518 21 (1970) 141–162. <https://doi.org/10.1146/annurev.pp.21.060170.001041>.
- 519 [46] K.A. van Leeuwen, P.D. Prenzler, D. Ryan, F. Camin, Gas Chromatography-Combustion-  
520 Isotope Ratio Mass Spectrometry for Traceability and Authenticity in Foods and  
521 Beverages: GC-C-IRMS for authentication in foods..., *Compr. Rev. Food Sci. Food Saf.* 13  
522 (2014) 814–837. <https://doi.org/10.1111/1541-4337.12096>.
- 523 [47] J. Hoefs, *Stable Isotope Geochemistry*, 8th ed., Springer International Publishing, 2018.  
524 <https://doi.org/10.1007/978-3-319-78527-1>.

525

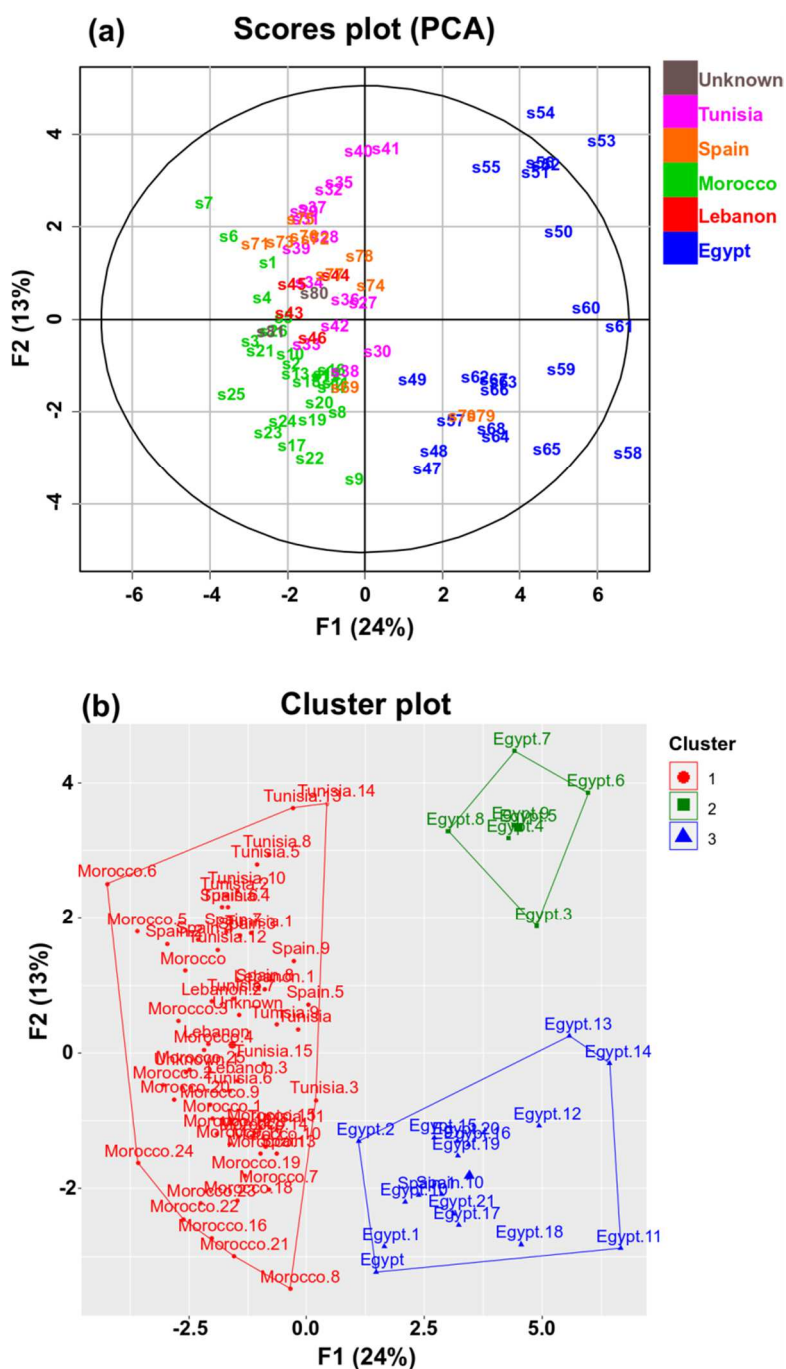
526



528 **Figure 1. (a)** Second dimension chromatographic profile obtained with MDGC (Columns HP-1  
 529 15m\*0.200mm\*0.5um. combined by Dean Switch system with a second column Cyclosil  $\beta$   
 530 30m\*0.250mm\*0.25um). This method enables the separation of 10 chiral metabolites:  $\alpha$ -  
 531 thujene 1(+), 2(-);  $\alpha$ -pinene 3(-), 4(+);  $\alpha$ -fenchene 5(+), 6(-); camphene 7(-), 8(+); sabinene 9(+),  
 532 10(-);  $\beta$ -pinene 11(+), 12(-);  $\alpha$ -phellandrene 13(-), 14(+);  $\delta$ -3-carene 15(+), 16(-); limonene 17(-  
 533 ), 18(+);  $\beta$ -phellandrene 19(-), 20(+). **(b)** Second dimension chromatographic profile obtained  
 534 with MDGC (HP-1 column 15m\*0.200mm\*0.5um, combined by Dean Switch system, with a  
 535 second column DEtTBuSilBetaCDX PS086 25m\*0.25mm\*0.25 $\mu$ m). This method enables the  
 536 separation of 7 chiral metabolites: linalool 21(+), 22(-); borneol 23(-), 24(+); terpinen-4-ol  
 537 25(+), 26(-);  $\alpha$ -terpineol 27(-), 28(+); linalyl acetate 29(+), 30(-). (Z)-nerolidol 31(+), 32(-); (E)-  
 538 nerolidol 33(-), 34(+).

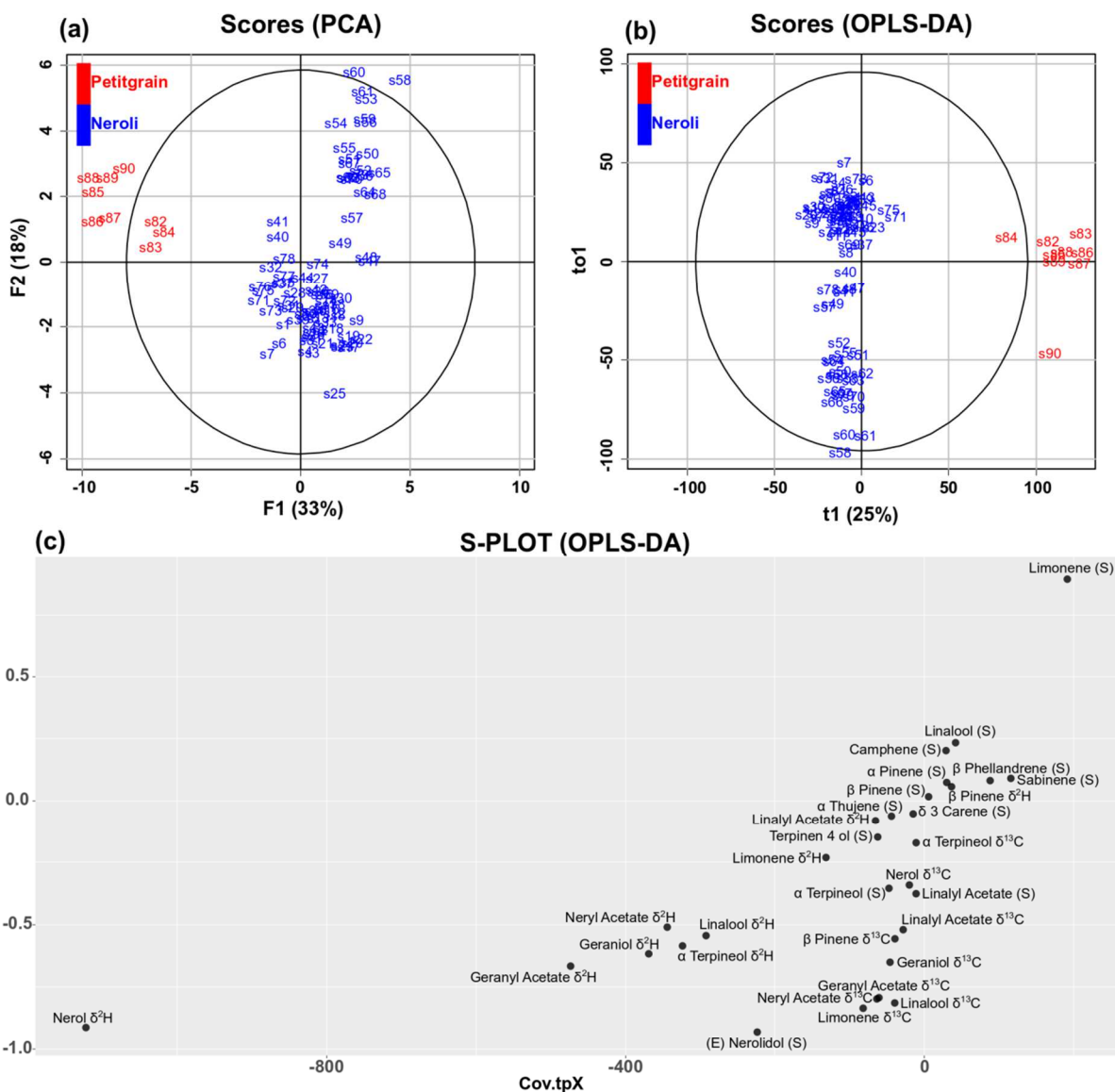
539



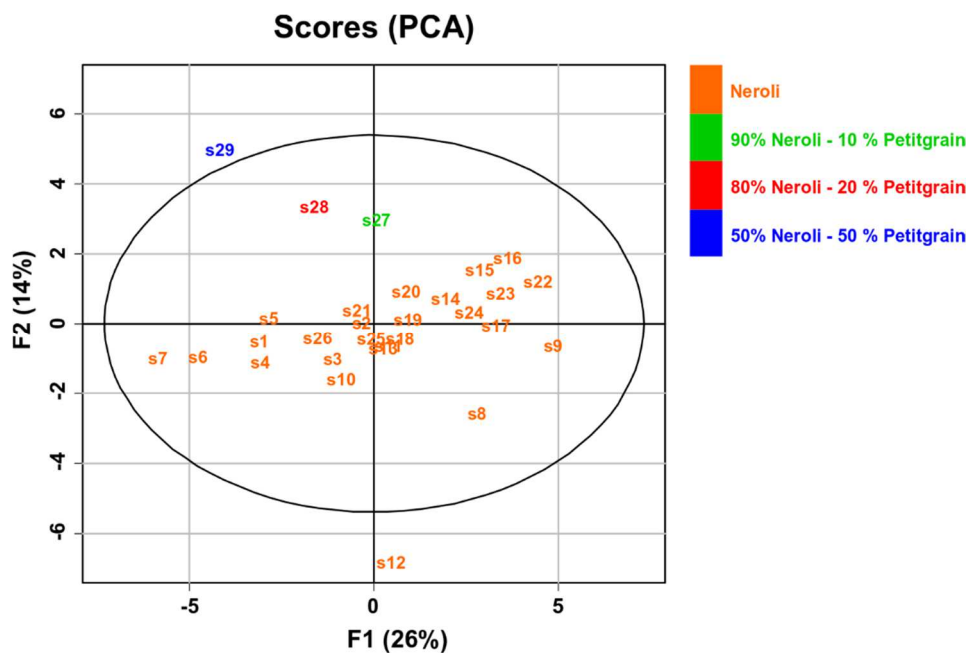


540  
 541 **Figure 2. (a)** Score plot of principal component F1 (24%) and F2 (13%) of Principal Component  
 542 Analysis (PCA) model developed from enantiomeric ratio percentages and  $\delta^{13}\text{C}$  and  $\delta^2\text{H}$   
 543 compound specific isotope analysis (CSIA) values determined on neroli essential oils from  
 544 different geographical origins: Morocco (in green), Egypt (in blue), Tunisia (in pink), Lebanon  
 545 (in red), and Spain (in orange). Samples with unknown geographical origins are represented in  
 546 grey. Clusters are represented via **(b)** hierarchical cluster plot. Cluster 1 (in red) includes

- 547 Moroccan, Lebanese, Tunisian, and most Spanish samples. Cluster 2 (in green) includes only
- 548 Egyptian samples. Cluster 3 (in blue) comprises some Egyptian and two Spanish samples.



549  
 550 **Figure 3. (a)** Score plot of principal component t1 (33%) and t2 (18%) of Principal Component  
 551 Analysis (PCA) model developed from enantiomeric ratio percentages and  $\delta^{13}\text{C}$  and  $\delta^2\text{H}$   
 552 compound specific isotope analysis (CSIA) values determined on neroli (in blue) and petitgrain  
 553 (in red) essential oils. **(b)** Orthogonal Partial Least Square – Discriminant Analysis (OPLS-DA)  
 554 score plot of enantiomeric ratio percentages and  $\delta^{13}\text{C}$  and  $\delta^2\text{H}$  CSIA values. **(c)** OPLS-DA  
 555 loadings S-Plot. This representation shows the correlation against the covariance.



556

557 **Figure 4.** Principal Component Analysis representation of the addition of petitgrain in neroli  
 558 essential oil. Three levels of adulteration were undertaken: 10% (green), 20% (red), and 50%  
 559 (blue) additions of petitgrain in 100% pure and natural Moroccan neroli essential oils (Samples  
 560 represented in orange).

561

**Table 1:** Enantiomeric distribution of chiral secondary metabolites of neroli and petitgrain essential oils from different geographical origins: Morocco, Tunisia, Lebanon, Egypt, Spain, Madagascar, and Paraguay.

Essential oil type	Geographical origin	Number of Samples	Enantiomeric distribution (%)																											
			$\alpha$ -Thujene S-(+)		$\alpha$ -Pinene S-(-)		Camphene 1S, 4R-(-)		Sabinene S-(-)		$\beta$ -Pinene S-(-)		$\delta$ -3-Carene 1S-(+)		Limonene S-(-)		$\beta$ -Phellandrene S-(+)		Linalool S-(+)		Terpinen-4-ol S-(+)		$\alpha$ -Terpineol S-(-)		Linalyl Acetate S-(+)		(E)-Nerolidol S			
			Mean	SD	Mean	SD	Mean	SD	Mean	SD	Mean	SD	Mean	SD	Mean	SD	Mean	SD	Mean	SD	Mean	SD	Mean	SD	Mean	SD	Mean	SD	Mean	SD
Neroli	Morocco	26	0.0	0.0	87.9	2.5	98.6	1.0	93.3	6.9	99.2	1.9	0.6	2.9	1.9	1.0	25.8	10.8	26.7	1.4	35.7	1.8	30.8	1.3	1.9	0.9	98.6	0.4		
Neroli	Tunisia	16	3.3	6.9	88.9	3.1	97.9	1.3	79.5	16.4	99.1	1.0	9.6	16.6	2.6	0.9	23.6	14.0	23.0	1.3	40.4	5.2	31.9	0.9	1.2	0.4	98.2	0.4		
Neroli	Lebanon	4	0.0	0.0	90.8	2.6	100.0	0.0	95.4	0.8	99.8	0.1	11.3	22.7	1.7	0.3	27.3	15.2	20.7	1.2	36.6	1.4	30.0	0.4	1.4	0.4	98.8	0.2		
Neroli	Egypt	22	23.4	26.7	65.9	9.6	94.3	6.1	24.9	20.8	94.6	17.3	0.3	1.1	2.5	0.6	53.1	18.1	18.6	4.0	59.8	6.2	32.5	6.2	0.7	0.1	97.5	1.5		
Neroli	Spain	11	12.0	26.7	86.5	9.5	97.7	3.5	77.1	30.9	99.5	0.8	0.0	0.0	2.2	0.8	40.0	18.3	28.2	3.4	42.7	9.9	29.7	2.5	1.4	0.3	98.4	1.0		
Petitgrain	Madagascar	3	0.0	0.0	92.7	3.0	100.0	0.0	92.0	0.6	98.2	0.9	0.0	0.0	9.2	2.8	18.3	16.7	24.4	4.3	30.9	7.8	27.6	1.2	0.4	0.3	81.0	5.5		
Petitgrain	Paraguay	6	5.5	6.1	81.0	4.4	100.0	0.0	73.9	27.7	98.4	0.6	0.9	0.8	24.0	2.3	53.5	4.9	28.1	3.4	42.3	10.2	27.0	0.2	0.4	0.2	77.0	6.2		

**Table 2:** Stable isotope  $\delta^{13}\text{C}$  distribution of secondary metabolites of neroli and petitgrain essential oils from different geographical origins: Morocco, Tunisia, Lebanon, Egypt, Spain, Madagascar, and Paraguay.

Essential oil type	Geographical origin	Number of Samples	Isotopic Distribution (‰)																			
			$\beta$ -Pinene $\delta^{13}\text{C}$		Limonene $\delta^{13}\text{C}$		Linalool $\delta^{13}\text{C}$		Linalyl Acetate $\delta^{13}\text{C}$		$\alpha$ -Terpineol $\delta^{13}\text{C}$		Neryl Acetate $\delta^{13}\text{C}$		Gernayl Acetate $\delta^{13}\text{C}$		Nerol $\delta^{13}\text{C}$		Geraniol $\delta^{13}\text{C}$		(E) Nerolidol $\delta^{13}\text{C}$	
			Mean	SD	Mean	SD	Mean	SD	Mean	SD	Mean	SD	Mean	SD	Mean	SD	Mean	SD	Mean	SD	Mean	SD
Neroli	Morocco	26	-26.32	0.97	-26.77	1.20	-25.47	0.95	-25.08	1.19	-26.64	1.90	-27.96	0.88	-26.77	0.98	-26.35	1.13	-26.58	0.78	-29.64	2.05
Neroli	Tunisia	16	-26.99	2.32	-27.33	1.02	-26.03	0.47	-26.15	1.23	-26.99	2.19	-29.30	2.01	-28.87	1.31	-27.39	1.36	-28.09	2.33	-30.65	2.45
Neroli	Lebanon	4	-26.99	1.08	-27.83	0.63	-26.37	0.65	-25.54	0.35	-28.10	1.69	-28.41	0.42	-27.38	0.60	-27.18	0.51	-27.19	0.75	-29.44	0.65
Neroli	Egypt	22	-26.71	1.57	-27.54	1.19	-25.96	0.88	-26.35	0.84	-27.88	1.54	-28.68	0.77	-27.67	0.89	-26.45	1.70	-27.02	1.00	-29.03	0.73
Neroli	Spain	11	-27.29	0.87	-28.31	0.94	-26.85	0.35	-27.54	1.24	-28.39	0.72	-28.99	0.72	-28.42	0.61	-27.17	0.80	-28.63	1.48	-27.98	1.17
Petitgrain	Madagascar	3	-28.01	1.31	-35.52	0.60	-29.73	0.21	-29.43	0.36	-28.31	0.08	-33.80	1.14	-33.38	0.82	-27.98	3.07	-30.77	0.47	N/A	N/A
Petitgrain	Paraguay	6	-31.51	2.92	-34.21	2.97	-29.48	0.23	-28.40	0.57	-28.21	1.68	-34.20	0.51	-32.89	0.85	-28.62	1.37	-31.99	1.16	N/A	N/A

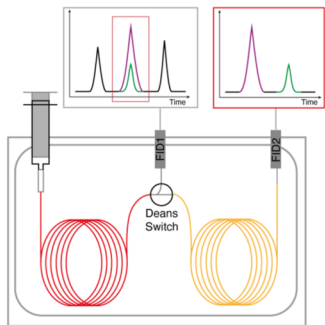
**Table 3:** Stable isotope  $\delta^2\text{H}$  distribution of secondary metabolites of neroli and petitgrain essential oils from different geographical origins: Morocco, Tunisia, Lebanon, Egypt, Spain, Madagascar, and Paraguay.

Essential oil type	Geographical origin	Number of Samples	Isotopic Distribution (‰)																			
			$\beta$ -Pinene $\delta^2\text{H}$		Limonene $\delta^2\text{H}$		Linalool $\delta^2\text{H}$		Linalyl Acetate $\delta^2\text{H}$		$\alpha$ -Terpineol $\delta^2\text{H}$		Neryl Acetate $\delta^2\text{H}$		Geranyl Acetate $\delta^2\text{H}$		Nerol $\delta^2\text{H}$		Geraniol $\delta^2\text{H}$		(E) Nerolidol $\delta^2\text{H}$	
			Mean	SD	Mean	SD	Mean	SD	Mean	SD	Mean	SD	Mean	SD	Mean	SD	Mean	SD	Mean	SD	Mean	SD
Neroli	Morocco	26	-213	12	-221	12	-210	7	-223	24	-224	12	-210	9	-203	14	-196	11	-201	11	-102	8
Neroli	Tunisia	16	-214	12	-223	8	-210	6	-237	17	-228	15	-208	11	-204	10	-189	9	-204	15	-106	8
Neroli	Lebanon	4	-218	4	-229	5	-209	7	-227	3	-222	5	-202	8	-203	16	-198	7	-205	4	-103	4
Neroli	Egypt	22	-208	32	-216	17	-199	16	-217	15	-217	14	-187	16	-182	9	-177	15	-188	9	-84	11
Neroli	Spain	11	-211	6	-212	21	-210	16	-220	32	-223	7	-214	11	-205	12	-198	17	-194	10	-101	14
Petitgrain	Madagascar	3	-212	15	-217	3	-219	5	-212	6	-239	3	-221	3	-229	2	-271	14	-220	1	N/A	N/A
Petitgrain	Paraguay	6	-205	4	-239	10	-239	5	-240	8	-255	4	-240	5	-241	4	-291	12	-232	17	N/A	N/A

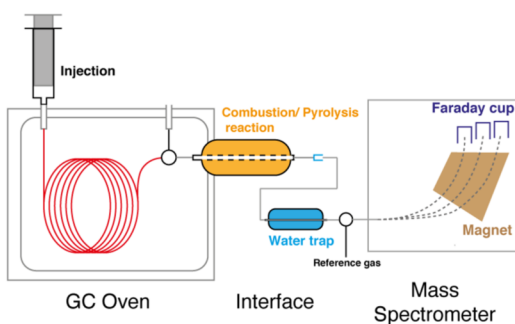
# Neroli essential oil sample



## Enantiomeric and Stable Isotope Ratio Fingerprints



**Enantio-MDGC**

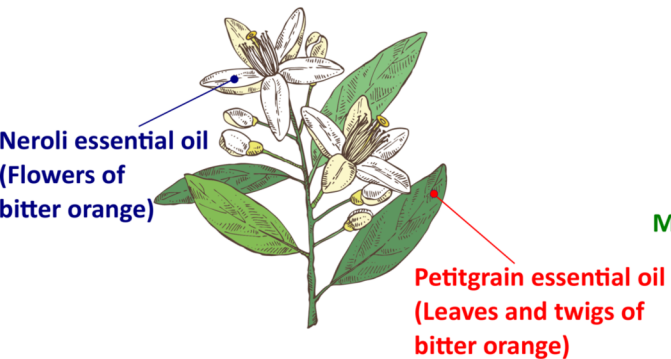


**GC-C/P-IRMS**



## Chemometric models

### Purity authentication



### Geographical differentiation

